DETERMINATION OF DYNAMIC RECRYSTALLIZATION PROCESS BY EQUIVALENT STRAIN

Xiaomei Qin[1], Wei Deng[2]
[1,2]Nanjing Iron& Steel Co.,LTD; Liuhe District, Nanjing,Jiangsu, 210035, China

Keywords: Equivalent strain, Dynamic recrystallization, Critical strain

Abstract

Based on Тарновский's displacement field, equivalent strain expression was derived. And according to the dynamic recrystallization (DRX) critical strain, DRX process was determined by equivalent strain. It was found that equivalent strain distribution in deformed specimen is inhomogeneous, and it increases with increasing true strain. Under a certain true strain, equivalent strains at the center, demisemi radius or on tangential plane just below the surface of the specimen are higher than the true strain. Thus, micrographs at those positions can not exactly reflect the true microstructures under the certain true strain. With increasing strain rate, the initial and finish time of DRX decrease. The frozen microstructures of 20Mn23AlV steel with the experimental condition validate the feasibility of predicting DRX process by equivalent strain.

Introduction

DRX is an important mechanism for the microstructure control during hot deformation. DRX plays a major role in reducing the flow stress and the grain size and is a powerful tool for controlling mechanical properties during industrial processing [1,2]. However, at present, laborious experimentations are needed to reveal kinetics for DRX, because that kinetics are measured by analyzing images of the frozen microstructures for different amounts of plastic deformation and levels of temperature obtained by single-pass hot compression tests [3-5]. Then, the kinetics for DRX are less well understood for most of the alloys formed by hot metal forming, although the kinetics for metallurgical behavior are strongly recommended to realize the numerical analysis of microstructure evolution in hot forming. This promotes the development of practical and precise methods to estimate the kinetics for DRX in a shorter time and requiring a lesser number of experiments.

The previous studies investigated DRX are almost by physical metallurgical methods [1-5], no researchers have proposed mathematical equivalent strain relations to determine the process of DRX. A new method to estimate the process of DRX by equivalent strain is proposed in this paper. The mathematical formulation of the method is explained in the following sections. Taking the DRX process of 20Mn23AlV steel as an example, the feasibility of predicting DRX process by equivalent strain are then validated.

Experimental Procedure and Mathematical Formulation

Experimental procedure: The chemical composition (wt.%) of the steel investigated was 0.2C,

23Mn, 2Al, 0.15Si, 0.1V and balance Fe. Specimens with a gauge length of 12mm and diameter of 8mm were machined from the as-received plates. The compressed deformation tests were performed on MMS-300 simulator equipment. The temperature was monitored by two thermocouples welded on the center of the specimen. As shown in Fig.1.
The specimens for metallographic examination were mechanically polished and etched, and then were observed by using LEICA DM2500M optical microscopy.

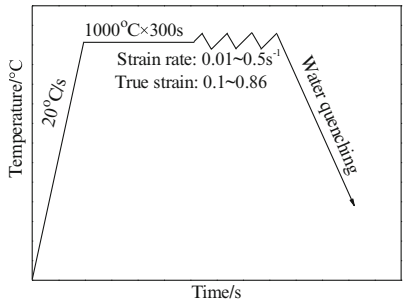

Figure 1 Schematic illustration of single-pass compression test

Derivation of equivalent strain: After compression, the macrograph of the specimens is shown in Fig.2(b). Because each specimen emerges bulge during compression, the deformation process can be simplified as Fig.2 (a) and (b). In Fig.2, x direction is parallel to radius direction of the specimen and y direction is parallel to compression direction. Deformation zone of cylinder compression is depicted as Fig.2 (c), because of symmetry, only one fourth of the deformation zone is taken into account. Тарновский gave the following displacement field [6]:

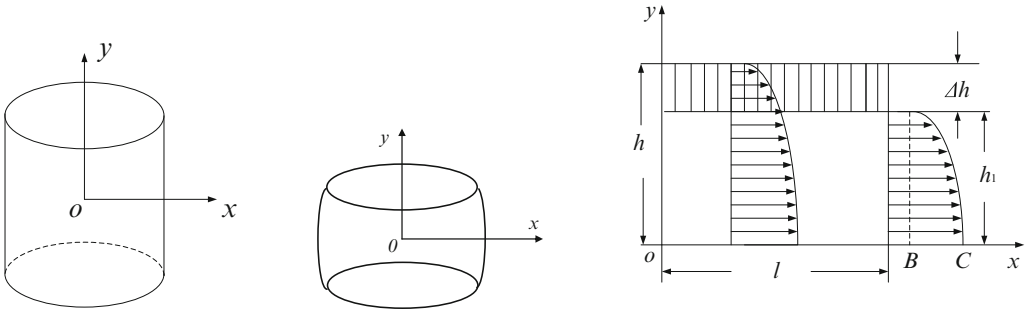

(a) Before compression (b) After compression (c) Displacement field

Figure 2 Coordinates and displacement field

$$\begin{cases} u_x = a_0 x + ax\left(1-\dfrac{3y^2}{h^2}\right)\left(1-\dfrac{1}{3}\dfrac{x^2}{l^2}\right) \\ u_y = -\left[a_0 y + ay\left(1-\dfrac{y^2}{h^2}\right)\left(1-\dfrac{x^2}{l^2}\right)\right] \end{cases} \tag{1}$$

Where u_x and u_y are displacement components in x and y directions; h and l are half height and radius of the specimen; a and a_0 are undetermined parameters, and $a_0=\varepsilon$, $a=\dfrac{b}{2l}-0.75\left(\dfrac{\Delta h}{h_1}-\varepsilon\right)$ [8], where h_1 is half height of the specimen after compression, $\Delta h=h-h_1$,

$\varepsilon=\Delta h/h$ and b is the length of $\overline{BC}$ (in Fig. 2c).

According to Cauchy Equation, the strain components from Eqn. (1) are:

$$\begin{cases} \varepsilon_x = a_0 + a\left(1-\dfrac{3y^2}{h^2}\right)\left(1-\dfrac{x^2}{l^2}\right) = -\varepsilon_y \\ \varepsilon_{xy} = -3a\dfrac{xy}{h^2}\left(1-\dfrac{x^2}{3l^2}\right) + a\dfrac{xy}{l^2}\left(1-\dfrac{y^2}{h^2}\right) \\ \varepsilon_{xz} = \varepsilon_{zy} = 0 \end{cases} \tag{2}$$

Where ε_x and ε_y are strain components in x and y directions.

For an arbitrary position in deformation zone, its equivalent strain is as follows [7]:

$$\varepsilon_e = \sqrt{\frac{2}{9}\left[\left(\varepsilon_x-\varepsilon_y\right)^2+\left(\varepsilon_y-\varepsilon_z\right)^2+\left(\varepsilon_z-\varepsilon_x\right)^2+6\left(\varepsilon_{xy}^2+\varepsilon_{yz}^2+\varepsilon_{zx}^2\right)\right]}$$

$$=9a^2\frac{x^2y^2}{h^4}\left(1-\frac{2x^2}{3l^2}+\frac{x^4}{9l^4}\right)-6a^2\frac{x^2y^2}{h^2l^2}\left(1-\frac{y^2}{h^2}-\frac{x^2}{3l^2}+\frac{x^2}{3l^2}\frac{y^2}{h^2}\right)+a^2\frac{x^2y^2}{l^4}\left(1-\frac{2y^2}{h^2}+\frac{y^4}{h^4}\right) \tag{3}$$

Substituting the values of h, l and a into Eqn.(3), equivalent strain in the whole deformation zone can be obtained.

The equivalent strain rate can be calculated as follows, $\dot{\varepsilon}_e = \dfrac{\varepsilon_e}{t}$ (4)

Where t is deformation time, and $t=\dfrac{\varepsilon}{\dot{\varepsilon}}$ ($\dot{\varepsilon}$ is strain rate of deformation).

Results and Discussion

Determination of dynamic recrystallizated critical strain: The effect of strain rate on the true strain–true stress curves of 20Mn23AlV steel investigated is shown in Fig. 3.

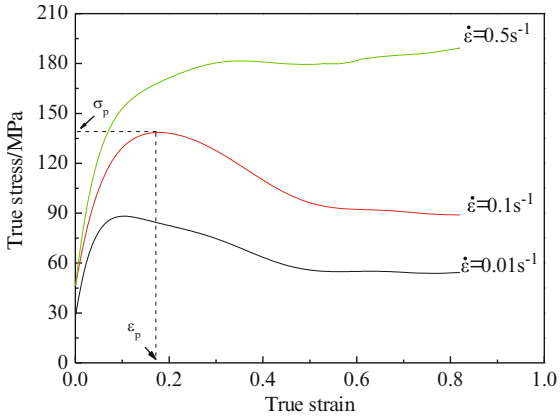

Figure 3 True stress–true strain curves of 20Mn23AlV steel under different strain rates at 1000℃

($\dot{\varepsilon}$ is strain rate)

For the flow stress curves given in Fig. 3, the true stress–true strain data were used to calculate the values of the strain hardening rate ($\theta=d\sigma/d\varepsilon$). According to the method to determine the critical point of DRX put forward by Poliak and Jonas [8-10] based on

irreversible consideration of thermodynamics, the calculated DRX parameters of critical stress and strain are listed in Table 1. It is obvious that with deformation temperature of 1000℃, the mentioned parameters increase with increasing strain rate.

Table 1 Calculated DRX parameters of 20Mn23AlV steel with different strain rates at 1000℃

Strain rate, s^{-1}	Critical stress, MPa	Critical strain
0.01	75.275	0.042
0.1	122.273	0.081
0.5	171.195	0.198

Distribution of equivalent strain and strain rate in deformed specimens: According to Eqns.(3) and (4), equivalent strain and strain rate distribution in different reduction specimens can be obtained. Fig.4 illustrates the contour maps of equivalent strain in specimens with true strain of 0.1, 0.4 and 0.6 (reduction ratio is 9.5%, 33% and 45%, respectively). The contour maps obvious reveal that equivalent strain distributions in all deformed specimens are inhomogeneous, the equivalent strain values in the center of the specimens (where l=0 and h=0, is defined as PA) are the largest, and those in the middle of die contact surface (where l=0 and h=6, is defined as PB) are the smallest.

Fig.5 indicates that the relationship of equivalent strain and equivalent strain rate in different portions inside specimens increases with increasing true strain, as deformation temperature is 1000℃ and strain rate is 0.1 s^{-1}. As shown in Fig.5 (b), equivalent strain rate changes slightly in that procedure. With true strain of 0.1, 0.4 and 0.6, the differences of equivalent strain between PA and PB are 0.074, 0.248 and 0.21, and the differences of equivalent strain rate are 0.074, 0.062 and 0.01 s^{-1}, respectively. With the help of parameters in Table 1, using interpolation method to determine the difference of critical strain between PA and PB is about 0.025 as deformation temperature is 1000℃ strain is 0.1 and strain rate is 0.1 s^{-1}, and with increase of strain and strain rate, the difference will smaller. Thus, in the determination process of DRX by equivalent strain in the paper, strain rate is assumed uniform throughout the entire specimen.

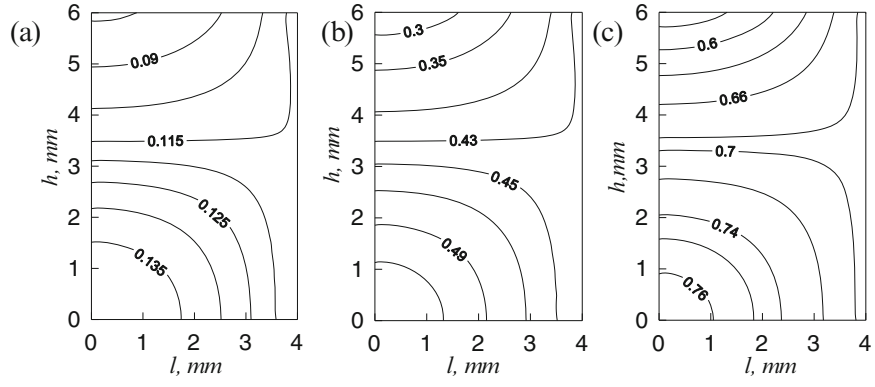

Figure 4 Contour maps of equivalent strain in samples with true strain of 0.1(a), 0.4(b) and 0.6(c), respectively

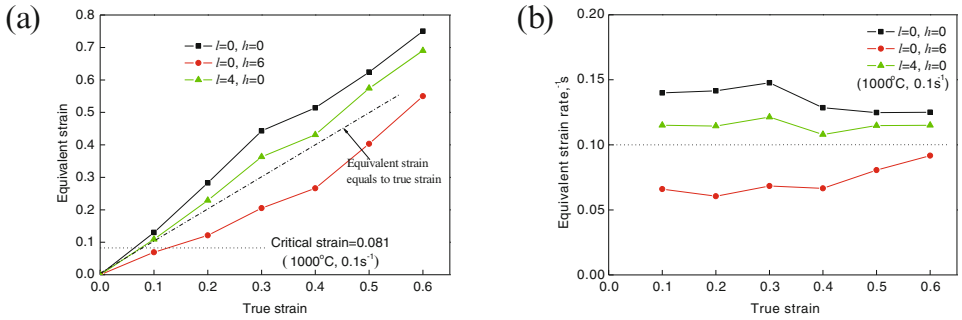

Figure 5 Relationships of equivalent strain (a) and equivalent strain rate (b) in different sites inside samples with increasing true strain

In previous researches about observation of dynamic recrystallization microstructure, some micrographs were taken at the center of the specimens or on tangential planes just below the surface [5,11], and some researchers did not explain where the micrographs were taken [12,13]. According to Fig.5, under a certain true strain, equivalent strain at the center or demisemi radius of the specimen are much higher than the true strain, and that on tangential plane just below the surface is larger than the true strain, too. Thus, micrographs at those positions can not exactly reflect the true microstructures under the certain true strain.

Application of equivalent strain in DRX: The initial time (R_s) and finish time (R_f) of DRX can be calculated by equations which were proposed by Akben et al [14]:

$$\begin{cases} R_s = \varepsilon_p / \dot{\varepsilon} \\ R_f = \varepsilon_f / \dot{\varepsilon} \end{cases} \tag{4}$$

Where ε_p is peak strain and ε_f is steady strain, they can be obtained from true stress-true strain curves.

Substituting ε_p, ε_f and $\dot{\varepsilon}$ into Eqn.(4), we can get the required time of DRX (R_t):

$$R_t = R_f - R \tag{5}$$

When the deformation temperature is 1000℃, R_t of 20Mn23AlV steel with different strain rates are listed in Table 2. The table shows R_t decreases with increasing strain rate.

Table2 R_t of 20Mn23AlV steel with different strain rates at 1000℃

$\dot{\varepsilon}$, s^{-1}	ε_p	ε_f	R_s, s	R_f, s	R_t, s
0.01	0.102	0.502	10.2	50.5	40.0
0.1	0.175	0.523	1.75	5.23	3.48
0.5	0.356	0.552	0.712	1.104	0.392

Take the deformation condition of 1000℃ and $0.1s^{-1}$ of 20Mn23AlV steel as an example. According to Table 1, under the condition, DRX critical strain of the tested steel is 0.081, viz., when equivalent strain in the steel increases to 0.081, DRX will start. In this case, as shown in Fig.6 (a), when the true strain are 0.06, 0.073 and 0.13, equivalent strain at the sites of PA, bulge (where l=4 and h=0, is defined as PC) and PB can reach 0.081, and those sites will initiate DRX. As can be seen in Table 2, R_t=3.48s, and true strain increment during this time is 0.348, thus, to finish DRX, the required true strain at the sites of PA, PC and PB are 0.408, 0.421 and 0.478, respectively.

In order to validate the feasibility of predicting DRX process by equivalent strain, the frozen

microstructures were obtained by the hot compression test with strain rate of $0.1s^{-1}$and true strain of 0.1, 0.4 and 0.6 at 1000℃. The frozen microstructures for different amounts of plastic strain (true strains are 0.1, 0.4 and 0.6) are shown in Fig. 6. Here, when the true strain is ε (0.1, 0.4 and 0.6), the sites of PA, PB and PC are represented by PA^{ε}、PB^{ε} and PC^{ε}, respectively.

As can be seen in Fig.5, with true strain is 0.1, the time of DRX has happened at the locations of $PA^{0.1}$ and $PC^{0.1}$ are 0.4s ($=\frac{0.1-0.06}{0.1s^{-1}}$) and 0.27s ($=\frac{0.1-0.073}{0.1s^{-1}}$), which are much lower than the time of DRX finished (R_t=3.48s), and at the same time, the equivalent strain at the site of $PB^{0.1}$ is 0.066, which has not reached the critical strain of DRX. Optical micrographs of $PA^{0.1}$, $PB^{0.1}$ and $PC^{0.1}$ are shown in Fig.6 (a)-(c). The microstructure in Fig.6(a) exhibits the DRX grain nuclei at the boundaries of deformed grains and only small proportion of DRX grains generate at $PA^{0.1}$. Fig.6(c) reveals the DRX is just beginning at $PC^{0.1}$, however, the microstructure in Fig.6(b) exhibits no DRX initiated at $PB^{0.1}$.

Similarly, according to Fig.5, we also can calculate the time of DRX has happened at the locations of $PA^{0.4}$, $PB^{0.4}$ and $PC^{0.4}$ are 3.4s, 2.7s and 3.27s, respectively. The microstructures in Fig.6 (d)-(f) reveal the DRX is nearly complete at $PA^{0.4}$ and $PC^{0.4}$, but incomplete at $PB^{0.4}$. For the locations of $PA^{0.6}$, $PB^{0.6}$ and $PC^{0.6}$, the calculated time of DRX has happened are 5.4s, 4.7s and 5.27s, respectively. Those are much larger than the time to complete DRX (R_t=3.48s). And the microstructures in Fig.6 (g)-(i) exhibit the equiaxial and fine grains demonstrating occurrence of complete DRX.

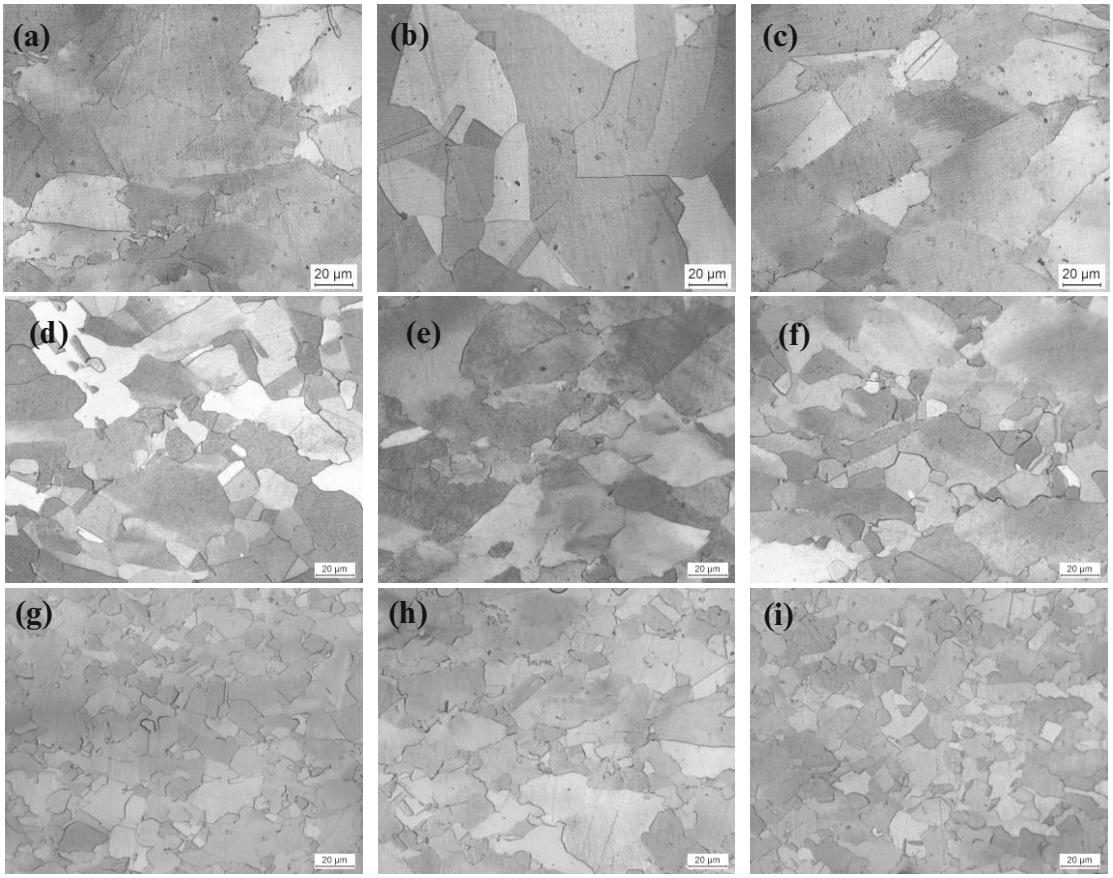

Figure 6 Optical micrographs of the tested steel at 1000℃with strain rate of $0.1s^{-1}$
(a) $PA^{0.1}$; (b) $PB^{0.1}$; (c) $PC^{0.1}$; (d) $PA^{0.4}$; (e) $PB^{0.4}$; (f) $PC^{0.4}$; (g) $PA^{0.6}$; (h) $PB^{0.6}$; (i) $PC^{0.6}$

Conclusions

(1) Equivalent strain distribution in deformed specimen is inhomogeneous, the equivalent strain value in the center of the specimen is the largest, and that in the middle of die contact surface is the smallest. Equivalent strain in the specimen increases with increasing true strain.
(2) Under a certain true strain, equivalent strains at the center or demisemi radius of the specimen are much higher than the true strain, and that on tangential plane just below the surface is larger than the true strain, too. Thus, micrographs at those positions can not exactly reflect the true microstructures under the certain true strain.
(3) The initiation and finish of DRX are time consuming. And with increasing strain rate, the initial and finish time of DRX decrease. With the conditions of strain rate of $0.1s^{-1}$ and true strain of 0.1, 0.4 and 0.6 at 1000℃, the frozen microstructures of 20Mn23AlV steel validate the feasibility of predicting DRX process by equivalent strain.

References

1. G.R. Stewart, J.J. Jonas, F. Montheillet, ISIJ Int. 44 (2004) 1581–1589.
2. F. Montheillet, J.J. Jonas, Encycl, Appl. Phys. 16 (1996) 205–211.
3. H.J. McQueen, S. Yue, N.D. Ryan, E. Fry, J. Mater. Process. Technol. 53 (1995) 293–310.
4. L.X. Du, Z.P. Zhang, G.F. She, X.H. Liu, G.D. WANG, J. Iron Steel Res. Int. 13 (2006) 31-35.
5. L.N. Pussegoda, J.J. Jonas, ISIJ Int. 31(1991) 278-288.
6. GD. Wang, D.W. Zhao, Modern Materials Forming Mechanics, frist ed., Northeastern University Press, Shenyang, 2004.
7. D.W. Zhao, Materials Forming Mechanics, first ed., Northeastern University Press, Shenyang, 2002.
8. E.I. Poliak, J.J. Jonas, Acta Mater. 44 (1996) 127-136.
9. E.I. Poliak, J.J. Jonas, ISIJ Int. 43 (2003) 684–691.
10. E.I. Poliak, J.J. Jonas, ISIJ Int. 43 (2003) 692–700.
11. B. Pereda, A. I. Fernández, B. López, J. M. Rodriguez-ibabe, ISIJ Int. 47 (2007) 860–868.
12. A.I. Fernández, P. Uranga, B. López, J.M. Rodriguez-Ibabe, Mater. Sci. Eng. 361 A (2003) 367–376.
13. M. E. Wahabi, L. Gavard, F. Montheillet, J.M. Cabrera, J.M. Prado, Acta Mater. 53 (2005) 4605–4612.
14. M.G Akben, B. Bacroix, J.J. Jonas, Acta Met. 31(1983) 161-174.